Yield Strength Increase of Cold Formed Sections Due to Cold Work of Forming

P. A. Sloof

R. M. Schuster

Fifteenth International Specialty Conference on Cold-Formed Steel Structures
St. Louis, Missouri U.S.A., October 19-20, 2000

Yield Strength Increase of Cold Formed Sections Due to Cold Work of Forming

P. A. Sloof[1], P.Eng. and R.M. Schuster[2], P.Eng.

Abstract

The design approach for predicting the increase in yield strength due to cold work of forming in the AISI 1996 Specification for the Design of Cold-Formed Steel Structural members is different from the approach used by the CSA Standard, CSA S136-94, Cold Formed Steel Structural Members. The AISI approach is based on the experimental work conducted by Karren and Winter, while the S136 approach is based on theoretical work by Lind and Schroff. Lind and Schroff used Karren and Winter's data to substantiate their theory. Karren and Winter conducted tests on five full sections and also collected strength data on the flat and corner elements of the same sections, allowing for comparison of tested to calculated values. Twelve different sections were tested as part of the University of Waterloo test program. Strength data was collected on virgin material, full sections and on the flat elements of formed sections, thus permitting comparisons to be made using only experimental data. The main purpose of this investigation was to help answer two questions, i.e., 1) should the average yield strength in the flats after forming be allowed in either design approach? and 2) is there a simplified expression that would produce similar results with fewer inputs? Based on the research of this paper, design recommendations were formulated.

1.0 Introduction

In design, the determination of the increase in yield strength due to cold work of forming gives rise for optimum utilisation of the structural capacity of cold formed steel members. The design of structures using cold formed steel members is governed by the American Iron and Steel Institute (AISI) 1996 Cold-Formed Specification [1] in the United States, and by CSA S136-94 [2] in Canada. Both of these design documents permit the strength increase due to cold work of forming in the determination of section or member capacities, but the method of determining this strength increase differs. Results can also differ, if the average yield strength of the flats after forming is used in the AISI method. The AISI method also uses a series of equations while S136 uses only one equation to calculate the yield strength. Based on these differences and the current efforts to develop a unified North American Specification for cold formed steel design, the following questions were addressed: 1), should the tested average yield strength of the flats after forming be allowed in the calculation of the yield strength due to cold work of forming? and 2), is there a simplified approach, which would produce similar results, that could be adopted regardless of the inclusion of the average yield strength of the flats after forming?

The primary objective of this research was to establish one consistent design approach for cold work of forming by using experimental test data. The scope of work included a review of previous work and a comparison of the current AISI and S136 design approaches of cold work of forming. In addition, a testing program consisting of tensile and compression tests of full sections was carried out along with testing of coupon specimens taken from the coils and the flats of the formed sections. The test results were used in a comparative analysis of the AISI and S136 design approaches.

1. Technical Manager, Vicwest Thermasteel Building Products, Oakville, Ontario Canada
2. Professor of Structural Engineering, Department of Civil Engineering and Architecture, University of Waterloo, Ontario, Canada

2.1 Development of AISI and S136 Design Approaches [3] [4]

The relevant metalurgical principles giving rise to cold work of forming are strain hardening, strain ageing and the Bauschinger effect. These phenomenom have their basis in plastic deformation, slip and dislocation movement and interaction at the atomic level. The effects are summarized in Figure 1, which shows a typical stress-strain relationship for a mild steel. Figure 1 also shows that if steel is loaded such that plastic deformation occurs (curve A to point B), is unloaded and then immediately reloaded again, there will be no change in the stress strain curve beyond point B; essentially, the curve will carry on from where it left off prior to unloading (segment C of curve). To this point the steel has undergone strain hardening. As indicated by curve D in Figure 1, strain ageing allows the recovery of the characteristic yield plateau but at stress values greater than after strain hardening. Strain ageing also increases the ultimate strength, but decreases the ductility. The Bauschinger effect can be described simply as the lower stress required to initiate plastic deformation in the direction opposite (reverse) to the original slip.

2.2 Effect of Cold Work of Forming on Cold Formed Sections

Research projects relating to the effects of cold work of forming, with specific emphasis on cold formed sections, began in the 1960's at Cornell University under the direction of Professor G. Winter, with the assistance of others [5] [6] [7]. The research included experimental work to investigate the effects of one-dimensional cold straining on sheet steels, and the effect of cold forming on the yield strength of flats and corners of sections and full section members. The results of the experimental work led to the publication of a number of important papers on the subject of cold work of forming. Based on the Cornell research, a design approach to predict the increase in yield strength due to cold work of forming was developed, and is currently used in the AISI Cold Formed Steel Specification[1]. Karren's work [6][7] led to the completion of analytical work by Lind and Schroff [8], resulting in a simplified design expression for predicting corner yield strengths. This simplified expression is currently being used in the CSA S136-94 Design Standard for Cold Formed Steel Structural Members [2].

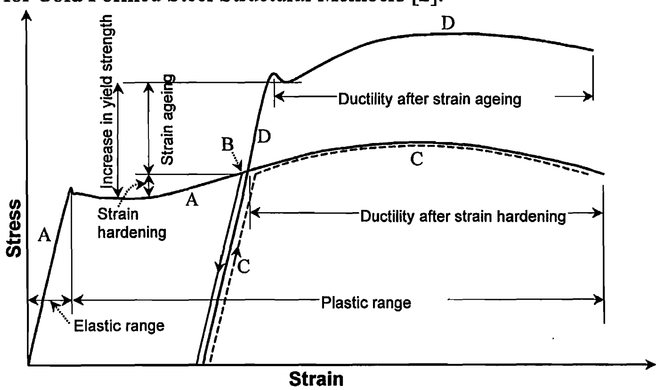

Figure 1 - Strain Hardening and Ageing of Mild Steel

2.3 Development of AISI Approach

The research completed by Karren and Winter at Cornell yielded significant results. Karren developed a theoretical expression for predicting the yield strength of a corner element after forming as:

$$\bar{\sigma} = \frac{kb}{(\frac{a}{t})^m} \tag{1}$$

Where b and m are empirical coefficients, a is the inside bend radius, t is the thickness and k is the strength coefficient. Two corner models were developed by Karren, each producing different expressions for b and m. In order to substantiate the validity of the model, coupon specimens taken from the corners and flats of formed sections were tested to determine the actual yield strength. The test results were in good agreement with the predicted values and showed that there was indeed a significant difference in the yield strength of the flats when compared to the corners, and the effect of cold work of forming was greatest at, and near, the corners. Karren postulated that the full section yield strength could be predicted using a weighted average of the corner and flat yield strengths as follows:

$$\sigma_{ys} = C\,\sigma_{yc} + (1 - C)\,\sigma_{yf} \tag{2}$$

where:
σ_{ys} = *full section yield strength*
σ_{yc} = *corner yield strength*
σ_{yf} = *yield strength of flats (from testing)*
C = *ratio of corner area to entire section area*

Tests were completed on full section specimens to substantiate this model. The results and comparisons are given in Table 1, where the tested virgin yield strength, tested full section yield strength, the calculated full section yield strength and the test-to-calculated ratios are given. The calculated full section yield strength was determined by using σ_{yf} *(from testing)* in Equation 2. The ratios indicate that there is close agreement between the calculated and the tested yield strengths.

Table 1 - Full Section Tested and Calculated Yield Strengths

Specimen Identification	Virgin Tensile Yield Strength ksi (MPa)	Flats Average Yield Strength ksi (MPa)	Full Section Tensile Yield from Tests ksi (MPa)	Calculated Full Section Yield ksi (MPa)	Ratio of Full Section Tensile Yield to Calculated
Hat (press braked cold reduced)	38.3 (264)	37.9 (261)	39.4 (272)	40.0 (276)	0.98
Hat (press braked hot rolled)	37.5 (259)	39.7 (274)	42.5 (293)	41.5 (286)	1.02
Track (Roll Formed hot rolled)	37.5 (259)	43.8 (302)	45.6 (314)	46.0 (317)	0.99
Channel (Roll Formed Hot rolled)	37.0 (255)	45.6 (314)	47.8 (330)	49.9 (344)	0.96
Joist Chord (Roll Formed Hot rolled)	30.7 (212)	46.8 (323)	50.0 (345)	50.6 (349)	0.99

Note: The a/t ratios of the sections in this table ranged from 0.89 to 1.49.

2.4 Computational Method

AISI [1] adopted the theory and equations developed by Karren and Winter [6][7], as the basis for calculating the average yield point of the full section due to cold work of forming. The AISI equations as presented in Section A7.2 are as follows:

$$F_{ya} = C\,F_{yc} + (1 - C)\,F_{yf} \tag{3}$$

Where:
F_{ya} = Average yield point of the steel in the full section of compression members or full flange sections of flexural members

C = For compression members, ratio of the total corner cross sectional area to the total cross-sectional area of the full section; for flexural members, ratio of the total corner cross-sectional area of the controlling flange to the full cross-sectional area of the controlling flange

F_{yf} = Weighted average tensile yield point for the flat portions established in accordance with Section F3.2 or virgin yield point if tests are not made

$F_{yc} = B_c F_{yv}/(R/t)^m$, tensile yield point of corners. This equation is applicable only when $F_{uv}/F_{yv} \geq 1.2$, $R/t \leq 7$, and the included angle $\leq 120°$.

B_c = $3.69\,(F_{uv}/F_{yv}) - 0.819(F_{uv}/F_{yv})^2 - 1.79$

m = $0.192\,(F_{uv}/F_{yv}) - 0.068$

R = inside bend radius

F_{yv} = Tensile yield point of virgin steel specified by Section A3 or established in accordance with Section F3.3

F_{uv} = Ultimate tensile strength of virgin steel specified by Section A3 or established in accordance with Section F3.3

2.5 Development of S136 Approach

Lind and Schroff [8], using Karren's [6][7] test data, developed an expression for predicting the corner yield strength and suggested that Karren's theory, "complicates and specializes the analysis and is not in good agreement with material behavior". In order to develop a less complicated method, they focused their analysis on a linear strain hardening law and a simplified design rule based on the "hardening margin", i.e., the difference between the virgin ultimate and yield strengths ($f_u - f_y$), and a strain hardening constant which would be the same for all materials. They explained their theory as follows: "The idea of the theory is simple. Whether a corner of a large or small radius is formed, the cold work, equal to the integral of the applied moment with respect to the angle of bend, should be about equal if strain hardening is linear. A small corner just concentrates the same work in a smaller volume of material. If the material hardens linearly, the work is independent of the radius, neglecting the elastic part. Further, if the increase in yield stress is a linear function of the work of forming, the increase in yield force for the corner will be a linear function of the work of forming". No testing was carried out, instead, Lind and Schroff used the experimental data produced from Karren's work[6][7] in the development of their theoretical linear strain hardening model. The data was used to establish the hardening constant, $5t$, and a simple design rule expressed as the increase in yield force as follows:

$$\Delta P = 5\,t^2\,(f_u - f_y)(\theta°/90°) \quad (4)$$

Essentially, the rule states that the yield strength is obtained by replacing the yield stress by the ultimate stress over an area $5t^2$ at each 90° corner. Equation 4 reflects the assumption that yield force is a linear function of work hardening and that if work hardening is linear then the increase in yield force is independent of the radius. The corner yield strength can therefore be calculated using the following equation:

$$F_{yc} = F_y + \Delta P/(\textit{area of corner}) \quad (5)$$

Lind and Schroff [8] compared calculations of the theoretical corner yield strengths with Karren's experimental results (in tension and compression) and found good agreement. A statistical analysis of the experimental divided by the calculated results produced a mean value of 1.008 with a standard deviation of 0.099, giving a coefficient of variation of 0.098. From this analysis, they noticed a systematic deviation of the ratios below 0.9 and suggested that the cause for this occurrence was the small inside bend radii associated with the specimens. Based on this, they stated that their expression tended to over estimate the corner yield strength for small inside bend radii. Their work shows that the increase in yield strength at a corner can be related to the strain hardening margin ($F_u - F_y$), and a strain hardening constant, *5t.* S136 [2] adopted their expression as the basis for calculating the yield strength due to cold work of forming. The method of calculating this yield strength is given in Clause 5.2 of S136 [2], as follows:

$$F_y' = F_y + 5\,D_A(F_u - F_y)/W^* \qquad (6)$$

Where:
F_y = Virgin yield strength of steel
D_A = Number of 90° corners or total number of degrees in the section divided by 90°
W^* = Ratio of centreline length of a flange cross-section of a member in bending, or of the entire cross section of a tensile or compressive member, to the thickness (w/t)
F_u = Ultimate yield strength of steel

2.6 Differences and Similarities of the AISI and S136 Approaches

The primary differences between the two design approaches are as follows:

1. Calculation of the average yield point for the full section in the AISI approach requires the use of several ancillary equations involving the radius, thickness, and the virgin steel mechanical properties F_{uv} and F_{yv}. In addition, the ratio of the total corner area to the entire section area, C, is required. Calculation of the yield strength, F_y', in the S136 approach requires the specified minimum yield and ultimate mechanical properties, the thickness, the number of corners and the centreline length of the section.
2. The AISI computation method contains a provision to allow the weighted average of the tested yield point values of the flats to be used for F_{yf} in Equation 3. S136 contains no such provision.
3. Different inside corner bend radii within a section are not accommodated in the AISI Specification.
4. Testing procedures are virtually identical with both approaches.
5. In both approaches, full section compressive and tensile testing can be used to determine the design yield stress (F_{ya} in AISI and F_y' in S136)

In addition to the above, a similarity exists in the structure and components of the principal predictor equations (Equations 3 and 6). Equation 6 can be rewritten as:

$$F_y' = \left(\frac{5D_a}{W^*}\right)F_u + \left(1 - \frac{5D_a}{W^*}\right)F_y \qquad (7)$$

In this form, it is clear that with the S136 approach a distinction is made between the contribution of the yield strength in the flats and the corners, as is the case with the AISI approach. However, when compared with Equation 3, F_u is replaced with F_{yc}, and F_y remains the same unless a value determined by testing of coupon specimens taken from the flats is used.

3.1 Waterloo Test Program [13]

The object of the Waterloo Test Program was to produce sufficient data on the mechanical properties of the steel in the virgin-unformed state and of the formed sections. This in turn would permit a comparison of measured to calculated values of the yield and ultimate strengths. Samples of cold formed steel structural members and virgin samples from the coil-steel, meeting strict fabrication criteria, were required and supplied by four different roll forming manufacturers. The shapes of samples produced for testing were Hat, C, lipped-C and U. Representative profiles are shown in Table 2 along with identification codes, material specifications and basic dimensions.

3.1.1 Material Requirement

In order to achieve the objectives described above, samples of cold formed steel structural members meeting certain criteria and virgin samples from the coil-steel were required. The coil-steel samples were to be taken from the same slit coil used to make the formed sections; two pieces were required, one immediately ahead of the formed section and one immediately behind. Figure 2 shows an illustration of this requirement. This technique helped to minimise the effects on the mechanical properties of distance-related variations along the coil.

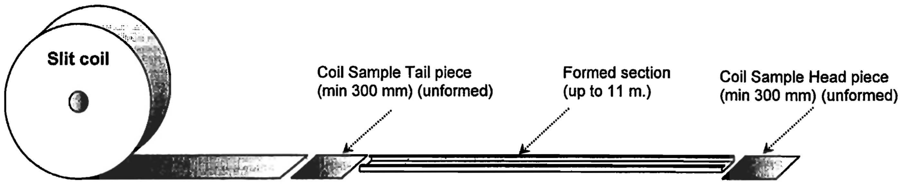

Figure 2 - Illustration of Material Requirement

The criteria for the formed sections were as follows:

1. The section had to be roll-formed (not brake-formed) using standard sheet steels. The section would not be an unusual shape, or one uncommonly encountered in the cold formed steel industry.
2. The section shape had to be such that the distribution of compressive stress in any element was uniform, i.e., no element could be subject to a significant area reduction.
3. The flange and web elements of the section had to be wide enough to provide at least one coupon for testing. No part of the section was to contain holes nor stiffeners.

3.1.2 Location of Specimens

In order to help reduce variations of mechanical properties due to length of sample, a specimen locating and cutting plan was established and used consistently throughout the test program. The samples submitted for testing were cut into sub-samples and each sub-sample was further divided into three sections. Each of these sections was then used to fabricate specimens. This plan is illustrated in Figure 3, which shows the sub-samples A, B, and C divided into sections to be used for stub column, flat element coupon and full section specimens. The specimen identification system shown in the figure was used to permit matching of the results upon completion of testing.

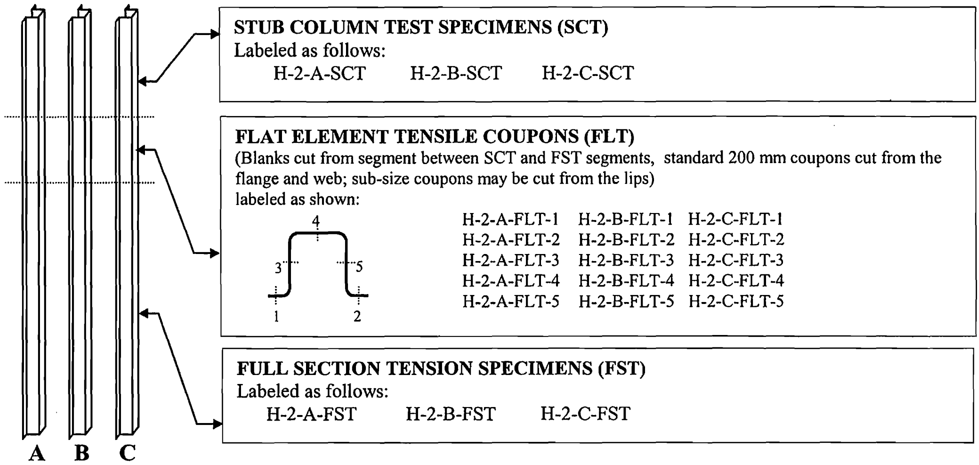

Figure 3 - Typical Specimen Cutting Plan

Table 2 - Sample Identification, Material Specifications and Dimensions

Id.	Material Specifications	Dimensions [in. (mm)] D	B	t	r	Profile
H-2	ASTM A653 grade 50 class 2 (345 MPa)	1.25(31.8)	1.62(41.1)	0.060(1.52)	0.063(1.60)	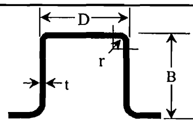
H-3	CSA G40.21-92 G230 (33 ksi)	1.33(33.7)	1.84(46.8)	0.056(1.41)	0.141(3.57)	
H-4	CSA G40.21-92 G230 (33 ksi)	1.50(38.1)	1.47(37.0)	0.058(1.47)	0.120(3.00)	
LC-1	ASTM A570 grade 33 (230 MPa)	1.65(42.0)	1.63(42.0)	0.103(2.61)	0.098(3.00)	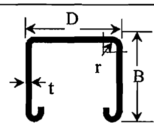
LC-2	ASTM A570 grade 33 (230 MPa)	1.64(41.6)	0.81(21.0)	0.074(1.89)	0.067(2.00)	
LC-3	ASTM A570 grade 33 (230 MPa)	1.65(42.0)	2.44(61.9)	0.100(2.54)	0.075(1.90)	
C-1	ASTM A607 grade 50 class 1 type 2 (345 MPa)	1.25(31.8)	1.62(41.0)	0.060(1.52)	0.189(5.0)	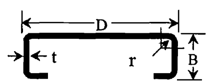
U-1	ASTM A607 grade 50 class 1 type 2 HSLAS (345 MPa)	2.99(76.0)	2.21(56.2)	0.074(1.88)	0.191(4.85)	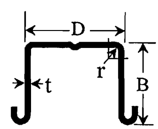
U-2		3.00(76.3)	2.19(55.7)	0.099(2.52)	0.218(5.54)	
U-3		3.94(100)	2.95(75.0)	0.110(2.80)	0.218(5.54)	
U-4		3.01(76.4)	2.97(75.4)	0.126(3.21)	0.249(6.33)	
U-5		4.02(102)	2.97(75.4)	0.126(3.21)	0.235(5.98)	

3.2 Tests

Tensile testing of coupon specimens and full section specimens was carried out in accordance with ASTM E 8M-98 Standard Test Methods for Tension Testing of Metallic Materials [Metric] [9]. Compressive testing of full section specimens was carried out using ASTM E 9 – 89a (Reapproved 1995) Standard Test Methods for Compressive Testing of Metallic Materials at Room Temperature [10]. Additional information regarding compressive testing was obtained from AISI Part VIII – Test Procedures [1]. Four different test types were carried out. The test types, specimen type, number of tests, the objective and the end use are described in Table 3.

Table 3 - Test Types and Use of Data

Test Type	Specimen Type	No. of Tests	Objective	End Use of Data
Virgin Tensile Test	Coupons (Tension)	72	To measure F_{yv} and F_{uv} of the steel directly from the coil prior to forming.	Calculation of m, B_c, F_{yc} and F_{ya} in AISI. Calculation of F_y' in S136.
Flats Tensile Test	Coupons (Tension)	192	To measure the yield and ultimate strength of the flat elements of a formed section.	Calculation of a weighted average yield strength, F_{yf}, of the formed section.
Full Section (compression)	Stub Column	36	To measure the ultimate load of a formed section in compression.	Comparison with calculated values (P/P_c) of a member in compression.
Full Section (tension)	Full Section with grip plates	36	To measure the tensile yield and ultimate load of a formed section in tension.	Comparison with calculated values (P/P_c) of a member in tension.

3.2.1 Virgin Material Coupon Tests

Standard coupon specimens were cut from the coil steel samples provided by the manufacturers. Three coupon blanks were cut from each head and tail coil sample in the longitudinal direction to the dimensions given in Figure 1 of ASTM E 8M [9]. The overall length of each coupon blank was 200 mm and the width was 20 mm. The reduced section length and width was 57 mm and 12.7 mm, respectively. Zinc galvanizing coatings were completely removed in a hydrochloric acid bath. An x-y plot, showing the load-elongation behavior, was created for each coupon specimen. All specimens exhibited sharp yielding characteristics and discontinuous yielding beyond the yield load. The yield strength was calculated using the load at yield and the original cross section area. The ultimate strength was calculated using the maximum load exerted on the specimen and the original cross-sectional area. All yield and ultimate strengths of the virgin material from the head and tail sections, the average of the two, and the ratio of F_{uv}/F_{yv}, are summarized in Table 4.

3.2.2 Flat Element Coupon Tests

Coupon blanks were cut from the flat elements of the samples between, or at the end of the stub column specimens and the full section tensile specimens. In situations where the flat element was not sufficient to cut standard sized coupons, as was the case of the lips of the hat sections, sub-size coupons were cut. Coupon blanks were cut from the centre of the flat elements in accordance with the ASTM , AISI and S136 documents describing the procedure to obtain the tensile yield strength of the flats. As shown in Figure 4, the shape of the load elongation curves typically varied from element to element. Some curves exhibited sharp yielding similar to the virgin test results, while others showed various degrees of gradual yielding. Variations of this type are an indication of the different degrees of cold work of forming that occurs in a formed section due to the section shape, sequence of roll stands and the number of steps required in forming. The yield load for coupon specimens with sharp yielding was taken as the upper yield load on yielding by the original cross-sectional area of the gage length. For gradual yielding specimens, the yield strength was established by using the 0.2% offset method. Elongation of the specimen was calculated by dividing the increase in distance between the gage markings by the original gage length. Weighted average yield and ultimate strengths for the flat elements F_{yfl} and F_{ufl} were established in accordance with Section F3.2 of the AISI Specification. A summary is given in Table 4.

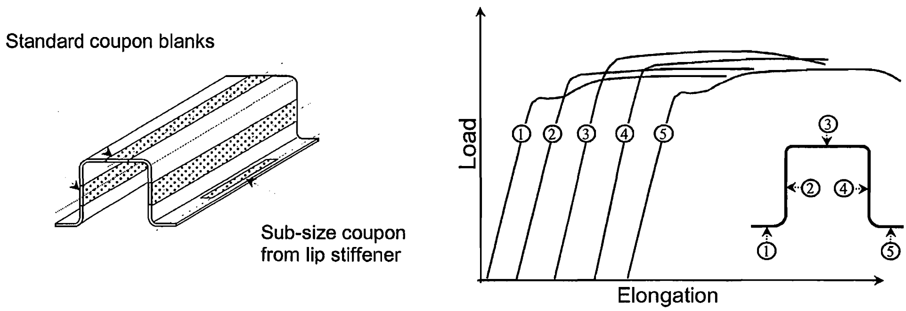

Figure 4 - Flat Element Coupon Locations and Typical Load Elongation Curves

Table 4 - Virgin Steel and Flat Element Yield Strengths

Sample Identification	**Average Virgin Yield and Ultimate Strength of Head and Tail Samples**			**Average (Weighted) Yield Strength of the Flats**
	F_{yv} ksi (MPa)	F_{uv} ksi (MPa)	F_{uv}/F_{yv}	ksi (MPa)
H-2	57.1 (394)	71.9 (496)	1.26	58.9 (406)
H-3	43.4 (299)	55.3 (381)	1.27	50.6 (349)
H-4	45.8 (316)	57.3 (395)	1.25	45.8 (316)
C-1	68.7 (474)	78.8 (543)	1.15	71.4 (492)
LC-1	44.2 (305)	58.4 (403)	1.32	51.3 (354)
LC-2	47.6 (328)	60.0 (414)	1.26	54.2 (374)
LC-3	40.8 (281)	57.9 (399)	1.42	43.7 (301)
U-1	64.8 (447)	76.6 (528)	1.18	72.2 (498)
U-2	65.4 (451)	80.8 (557)	1.24	69.8 (481)
U-3	59.5 (410)	75.3 (519)	1.27	64.5 (445)
U-4	68.3 (471)	80.6 (556)	1.18	72.2 (498)
U-5	59.5 (410)	81.4 (561)	1.37	61.5 (424)

1. Based on 50 mm gage length.

3.2.3 Full Section Compressive Tests

The ultimate compressive load of the full sections was determined by testing full section stub column specimens. Prior to testing, the specimens were checked for local buckling in accordance with Clause 5.6.2 of S136 [2]. Fabrication and testing was completed in accordance with the Test Procedures for use with the 1996 AISI Cold-Formed Steel Specification-Stub-Column Test Method [1].

The specimen length varied according to the section dimensions. In order to preclude the potential of

The specimen length varied according to the section dimensions. In order to preclude the potential of overall column-buckling, the relationship $3d < L < 20\ r_y$ was used to determine the length of each specimen. In this expression, L = the overall length of the specimen, r = radius of gyration about weak axis (typically y), and d = depth of section (measured parallel to web).

The results are summarized in Table 5. Buckling modes ranged from local buckling in the flat web and flange elements to lip/flange distortional buckling and flange/web distortional buckling [11] [12].

3.2.4 Full Section Tensile Tests

The tensile yield and ultimate strengths of the full section tests were established by testing specimens fabricated from full section members. Unfortunately, there was little information that addresses this type of testing directly, specifically with regards to fabrication of specimens. ASTM E 8M [9], the AISI Cold-Formed Specification [1], the work by Karren and Winter [7] and some trial and error work, provided guidance in this regard. In the end, two types of gripping methods were used. The machine used for this testing was equipped with wedge grips capable of clamping material up to 80 mm in thickness. The C and lipped-C section specimens were gripped directly in the wedge grips. A steel spacer block was inserted within the section to prevent collapse of the ends of the specimen. The remaining specimens were fabricated using steel plates welded to the flanges of the section. A solid steel grip tongue, was inserted into the end of the specimen and welded to the inside of the flanges. Two smaller plates (flange plates) were welded to the outside of the flanges and to the tongue. The tongue and plates were arranged around the center of gravity of the section. Overall specimen lengths were varied in accordance with the section dimensions. The grip tongue and flange plate lengths were varied depending on the amount of weld required. In each case, the distance between the welded flange plates at each end was at least $5D$. The overall length of the C and lipped-C sections was 750 mm, leaving approximately 550 mm between the upper and lower wedge grips.

All load elongation curves showed gradual yielding of the specimen and as a result the yield strength was established using the 0.2% offset method. The ultimate strength was calculated by dividing the maximum load by the cross sectional area. The percent elongation was also determined. The test results are summarized in Table 5. As loading increased, some specimens deflected laterally in a direction perpendicular to the web. This deflection was not measured but was estimated to be approximately 0.20 in. (5 mm) and commonly occurred after the yield load was reached. At failure, the specimen necked downward in the vicinity of the fracture region. Fracture almost always was initiated along the edge of the lip. Typical failed Hat section specimens are shown in Figure 5.

Table 5 - Stub Column and Full Section Tensile Test Results

Sample Identification	Stub Column Test P_{ult} kips (kN)	Full Section Tensile Test P_y kips (kN)	P_{ult} kips (kN)
H-2	20.1 (89.3)	20.4 (90.8)	23.8 (106)
H-3	15.9 (70.6)	16.7 (74.1)	19.1 (85.0)
H-4	15.8 (70.3)	15.7 (70.0)	19.0 (84.7)
C-1	31.5 (140)	32.8 (146)	35.7 (159)
LC-1	18.3 (81.4)	17.8 (79.3)	18.6 (82.7)
LC-2	33.0 (147)	34.6 (154)	41.4 (184)
LC-3	39.3 (175)	41.1 (183)	42.3 (188)
U-1	40.2 (179)	46.3 (206)	51.5 (229)
U-2	58.0 (258)	61.4 (273)	68.6 (305)
U-3	78.2 (348)	81.8 (364)	108.6 (483)
U-4	94.2 (419)	97.8 (435)	95.5 (425)
U-5	87.9 (391)	95.8 (426)	105.7 (470)

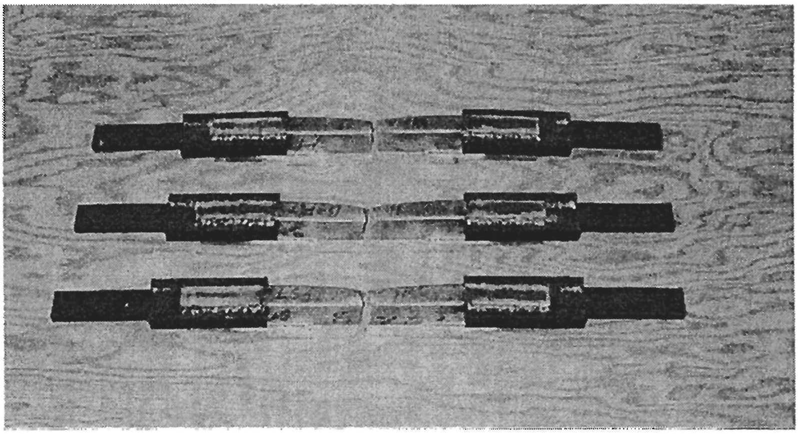

Figure 5 - Typical Failed Hat Section Tension Specimens

4.1 Analysis of Test Results [13]

The analysis was comprised of three parts. First, the yield strength increase of the flats, corners and full sections were compared with the results of Karren and Winter's [7] experimental work to identify similarities and differences. Second, the results were analyzed for the effect of the ratios, F_{uv}/F_{yv}, r/t, and the $(F_{uv} - F_{yv})$ margin regarding the change in yield strength of the flats, corners and full sections in comparison to the virgin yield strength of the material. Finally, compression and tension load ratios (tested versus calculated) were established to permit a comparison of the tested yield load to the calculated yield load and a comparison of the calculated results of each design approach (AISI and S136).

4.2 Comparison with Previous Experimental Work

The flat element test results showed that cold work of forming increased the average yield strength of the flats with only a few exceptions. These exceptions being several flanges and lips for the H-2, H-3 and H-4 sections, where it remained the same, or only decreased slightly. The results also showed, in accordance with Karren and Winter's experimental work [7], an element to element variation in the yield strength. This variation can be attributed largely to the way in which the section was roll formed, i.e., the number of roll stands, sequence of bending, etc, and to a lesser degree on the variation of the virgin mechanical properties across the width of the coil. Further information on the comparison of flat element test results can be found in reference 13.

4.2.1 Effect of F_{uv}/F_{yv} on Yield Strength

From Karren's [6] research of corner properties, in which he tested 226 specimens of various radius and virgin mechanical properties, he showed that virgin materials with high F_{uv}/F_{yv} ratios have a greater potential for strain hardening than materials with low ratios. In other words, the amount of yield strength increase due to cold work of forming increased as the F_{uv}/F_{yv} ratio increased. As shown in Table 4, the F_{uv}/F_{yv} ratio for the three groups with various steel grades ranged from 1.15 to 1.42. Three sections had an F_{uv}/F_{yv} ratio below 1.2; C-1 (1.15), U-1 (1.18) and U-4 (1.18). The mean F_{uv}/F_{yv} ratios for the Hat, lipped-C, and U sections were 1.23, 1.33 and 1.22, respectively, which shows a similar increase of yield strength as the ratio increases.

4.2.2 Effect of *r/t* ratio on Yield Strength

By varying the *r/t* ratio of his specimens, Karren [6] demonstrated that as the *r/t* ratio increased cold work of forming decreased. Karren varied both the material thickness and the inside bend radius of his specimens for all 226 specimens. The *r/t* ratios of the corner specimens used by Karren ranged from 0.71 to 6.32. The *r/t* ratio for the Waterloo test sections ranged from 0.75 to 2.58. The mean ratios for the Hat, lipped-C and U sections were 1.87, 0.86 and 2.12, respectively. The low *r/t* ratio for the lipped-C sections was due mainly to relatively small inside bend radii. The relationship between the increase in yield strength expressed as F_y/F_{yv} and the *r/t* ratio was demonstrated and shows good agreement with Karren's results.

4.2.3 Effect of ($F_{uv} - F_{yv}$) Margin on Yield Strength

Karren's [6] data of the increase in yield strength of corners was used by Lind and Schroff [8] in the development of the *5t* rule. Lind and Schroff did not disagree with Karren's conclusions, but demonstrated that a simpler method of approximating the increased yield strength existed. Using Karren's data of the 226 corner specimens, they were able to demonstrate that the yield strength after cold work of forming could be approximated by substituting the virgin ultimate strength for the virgin yield strength over a distance of *5t* at each corner. In addition to the F_{uv}/F_{yv} and *r/t* relationships noted above, they concluded that the yield strength increases were also related to the ($F_{uv} - F_{yv}$) margin. The Waterloo test results substantiated this conclusion.

4.3 Comparison of AISI and S136 Design Approaches

The comparison of the AISI [1] and S136 [2] approaches to cold work of forming was made on the basis of measured and calculated load resistances of fully effective members in compression and tension. Calculated load resistance values were taken as the product of the yield strength of a section using cold work of forming and the measured virgin mechanical properties to obtain F_{ya} or F_y', and the area of the section. Measured-to-calculated load ratios were then determined and analyzed. The analysis was completed separately for the stub column and the full section tensile specimens.

4.4 Method of Calculating Compression Load Ratios (P_t/P_c)

Measured-to-calculated compression load ratios P_t/P_c were calculated in five different ways. An explanation of the method of calculation is given in Table 6.

4.4.1 Local and Distortional Buckling

All sections were checked for the possibility of any significant effective area reduction due to local and/or distortional buckling. The sections were checked using Clause 5.6.2.3 of S136-94 [2] and using the minimum guaranteed yield strength given for the material. Small area reductions of less than 1.5% were found for the curved lip stiffeners of two of the sections and a third section showed an area reduction of less than 0.5 % in the simple lip stiffeners.

Table 6 - Explanation of Compressive Yield Load Calculations

Ratio	Description of Yield Load	Yield Load Calculation	Yield Stress Calculation
P_t/P_{yv}	P_{yv} is the load at which yielding of the specimen would occur without any influence from buckling (local, overall or distortional). No consideration was given to cold work of forming.	$P_{yv} = F_{yv} \times A_g$	F_{yv} (from tests)
P_t/P_{yeff}	P_{yeff} is the load at which yielding of the specimen would occur when local and/or distortional buckling is considered.	$P_{yeff} = F_{yv} \times A_{eff}$	F_{yv} (from tests) A_{eff} was determined using S136 Clause 5.6.2.3.
$P_t/P_{c(S136)}$	$P_{c(S136)}$ is an approximation of the load at which the fully effective section would yield when cold work of forming is considered in the S136 approach.	$P_{c(S136)} = F_y' \times A_g$	F_y' was calculated using Equation 6: $F_y' = F_y + 5\,D_A(F_u - F_y)/W^*$ $(W^* = w/t)$; $(F_y = F_{yv})$; $(F_u = F_{uv})$
$P_t/P_{c(AISI)}$	$P_{cf(AISI)}$ is an approximation of the load at which the fully effective section would yield when cold work of forming is considered in the AISI approach.	$P_{c(AISI)} = F_{ya} \times A_g$	F_{ya} calculated using Equation 3: $F_{ya} = C\,F_{yc} + (1 - C)\,F_{yf}$; Where F_{yf} is the yield strength of virgin material (prior to forming) determined through testing.
$P_t/P_{cf(AISI)}$	$P_{cf(AISI)}$ is an approximation of the load at which the fully effective section would yield when cold work of forming is considered in the AISI approach.	$P_{cf(AISI)} = F_{ya} \times A_g$	F_{ya} was calculated using Equation 3 as above, except F_{yf} was the yield strength of the flats determined through testing.

The sections were rechecked for area reductions using the virgin steel yield strength test results. Seven of the twelve sections required area reductions of up to 14%, due to reductions of the intermediate stiffener and edge stiffener areas.

The test results showed that distortional buckling of the flange about the flange/web corner and local buckling of the web was the most common mode of failure among the lipped-C , C and U sections. Local buckling was the predominant mode of failure in the hat sections. Both types of failure indicate that the effective area (A_{eff}) of the section was less than the gross area (A_g) at the failure load. For comparative purposes, the effective area was used to calculate the P_t/P_{yeff} ratio. Exclusion of A_{eff} from the remaining P_t/P_c ratios, produced more conservative results, that is, higher ratios. Provided this is done consistently, a valid comparison of the ratios can be made. Therefore, all other P_c values were calculated assuming a fully effective section.

4.5 Compression Load Ratio Comparisons

Average specimen test results, P_t, areas A_g and A_{eff}, and the measured-to-calculated load ratios of individual specimens and statistical summaries of the three groups and of all the specimens are summarized in Table 8. When using only measured virgin mechanical properties (F_{yv} and F_{uv}), the S136 and the AISI approaches for compressive resistance consistently produce results that are within 2% of each other when the section groups are considered as can be seen in Columns 3 and 4. If all sections are considered, as in the summary of all specimens, there is virtually no difference. Both approaches produce ratios lower than 1 for the U-shaped sections, indicating an over-estimation of the compressive load resistance. Although area reductions disallow the use of cold work of forming in both approaches, the use of effective areas in the compressive load calculations would have increased these load ratios.

The use of F_{yft} in the AISI approach caused a 4% decrease in the compressive load ratio of all specimens, shown in column 5 from the ratio shown in column 4, indicating that the calculated load was greater than the tested load, on average, by approximately 2%. The decrease was greatest for the Lipped-C sections and least for the Hat sections, but even with this decrease the ratios were 0.99 for the Hat sections and 1.03 for the Lipped Channel. However, in the case of the U sections, the load ratio was 0.94 indicating that the calculated compression load was over-estimated by approximately 6%. As noted above, the use of effective areas would have improved upon this condition.

4.6 Method of Calculating Tension Load Ratios (P_t/P_c)

Measured-to-calculated tension load ratios P_t/P_c were calculated in four different ways. An explanation of the method of calculation is given in Table 7.

4.6.1 Tension Load Ratio Comparisons

Measured-to-calculated load ratios of individual specimens and statistical summaries of the three groups and for all specimens are summarized in Table 9. The results show that using only measured virgin mechanical properties (F_{yv} and F_{uv}), the S136 and the AISI approaches for tensile resistance, (columns 2 and 3) consistently produce results that are within 2% of each other when the section groups are considered. In the summary of all specimens, the difference is less than 1%. The use of F_{yft} in the AISI approach (column 4) led to an overall decrease in the average ratio of all specimens to 1.02 and there was only a small difference of less than 2% between the average Hat, Lipped C and U section ratios.

It must be understood that the F_{yft} value used in this analysis was at the low end of the scale of possible values, since only one coupon was taken from each flat element and this coupon was taken from the middle of the element as shown in Figure 4. AISI allows as many coupons as the width will permit, as long as one coupon is taken from the middle. This technique will undoubtedly produce greater values for certain sections, and ultimately drive up the calculated yield strength due to cold work of forming.

Table 7 - Explanation of Tension Yield Load Calculations

Ratio	Description of Yield Load	Yield Load Calculation	Yield Stress Calculation
P_t/P_y	P_y is the load at which yielding of the specimen would occur without any influence from buckling (local, overall or distortional). No consideration was given to cold work of forming.	$P_y = F_y \, x \, A_g$	F_{yv} (from tests)
$P_t/P_{c(S136)}$	$P_{c(S136)}$ is an approximation of the load at which the fully effective section would yield when cold work of forming is considered in the S136 approach.	$P_{c(S136)} = F_y' \, x \, A_g$	F_y' was calculated using Equation 6: $F_y' = F_y + 5\,D_A(F_u - F_y)/W^*$ $(W^* = w/t);(F_u = F_{uv});(F_y = F_{yv})$
$P_t/P_{c(AISI)}$	$P_{cf(AISI)}$ is an approximation of the load at which the fully effective section would yield when cold work of forming is considered in the AISI approach.	$P_{c(AISI)} = F_{ya} \, x \, A_g$	F_{ya} was calculated using Equation 3: $F_{ya} = C\,F_{yc} + (1 - C)\,F_{yf}$ Where F_{yf} is the yield strength of virgin material (prior to forming) determined through testing.
$P_t/P_{cf(AISI)}$	$P_{cf(AISI)}$ is an approximation of the load at which the fully effective section would yield when cold work of forming is considered in the AISI approach.	$P_{cf(AISI)} = F_{ya} \, x \, A_g$	F_{ya} was calculated using Equation 3 as above, except F_{yf} was the yield strength of the flats determined through testing.

4.7 Waterloo Approach to Cold Work of Forming

The Waterloo approach was developed in response to the recognition of the small difference between the end result of the AISI and S136 approaches when virgin material properties are used and of the justification for inclusion of tested yield strength of the flats in the calculation. The simplicity of the S136 approach when compared to AISI was also a factor. Upon review of the results in Tables 8 and 9, it was clear that no appreciable difference exists between the calculated yield strengths of the AISI and S136 Approaches. This statement is true regardless of how the results are viewed, i.e., by specimen, section group or all sections, and also regardless of compressive or tensile loading. The test results also demonstrated that the inclusion of F_{yft} obtained by testing can be used in the AISI approach with satisfactory, albeit less conservative, results. The Waterloo approach considers both of these facets in its development.

It seemed reasonable to postulate that the use of tested flat element yield strengths in the S136 equation would produce similar results to the AISI equation, given that it was developed using Karren's data. Moreover, and perhaps not surprisingly, a similarity exists between the AISI equation and the rearranged S136 equation; each one essentially contains two components, i.e., one for the flats and one for the corners. Each equation produces a weighted-average yield strength for the section. The equation used in the Waterloo approach can be expressed as follows:

$$F_y' = \left(\frac{5\,D_a}{W^*}\right) F_u + \left(1 - \frac{5\,D_a}{W^*}\right) F_{yft} \qquad (8)$$

Where:

F_{yft} = weighted average yield strength of the flats determined from coupon tests.

The load ratios calculated using this equation are shown in column 6 of Table 8 for specimens in compression and column 5 in Table 9 for specimens in tension.

Table 8 - Comparison of Measured to Calculated Load Ratios of Compression Specimens

Specimen Identification	P_t (kN)	A_g (mm²)	A_{eff} (mm²)	P_t/P_y (1)	P_t/P_{yeff} (2)	$P_t/P_{c(S136)}$ (3)	$P_t/P_{c(AISI)}$ (4)	$P_t/P_{cf(AISI)}$ (5)	P_t/P_{wat} (6)
H-2	89.3	217	214	1.04	1.06	0.99	0.99	0.95	.96
H-3	70.6	216	216	1.09	1.09	1.04	1.03	0.99	1.00
H-4	70.3	208	207	1.06	1.07	1.01	1.01	1.00	1.01
C-1	175.7	342	342	1.10	1.09	1.04	1.03	0.99	1.01
Mean				**1.07**	**1.08**	**1.02**	**1.01**	**0.99**	**0.99**
Standard Deviation				**0.042**	**0.039**	**0.040**	**0.038**	**0.031**	**0.034**
Coefficient of Variation				**0.039**	**0.036**	**0.039**	**0.037**	**0.032**	**0.034**
LC-1	140.0	349	349	1.31	1.32	1.10	1.11	1.03	1.06
LC-2	81.4	183	183	1.35	1.36	1.18	1.18	1.08	1.12
LC-3	147.3	445	445	1.18	1.18	1.00	1.02	0.97	0.96
Mean				**1.28**	**1.28**	**1.09**	**1.10**	**1.03**	**1.05**
Standard Deviation				**0.082**	**0.083**	**0.079**	**0.070**	**0.051**	**0.070**
Coefficient of Variation				**0.064**	**0.065**	**0.072**	**0.063**	**0.050**	**0.067**
U-1	179.3	395	353	1.03	1.14	0.96	0.97	0.89	0.90
U-2	258.3	529	529	1.09	1.08	0.98	0.99	0.97	0.96
U-3	349.0	796	695	1.08	1.23	0.97	0.99	0.97	0.96
U-4	419.7	846	752	1.06	1.19	0.97	0.98	0.95	0.95
U-5	391.7	913	884	1.05	1.08	0.94	0.95	0.93	0.94
Mean				**1.06**	**1.14**	**0.97**	**0.98**	**0.94**	**0.94**
Standard Deviation				**0.029**	**0.062**	**0.019**	**0.020**	**0.033**	**0.029**
Coefficient Of Variation				**0.027**	**0.054**	**0.020**	**0.021**	**0.035**	**0.031**
Summary of All Specimens									
Mean				**1.12**	**1.16**	**1.02**	**1.02**	**0.98**	**0.99**
Standard Deviation				**0.107**	**0.100**	**0.067**	**0.066**	**0.050**	**0.060**
Coefficient Of Variation				**0.095**	**0.086**	**0.066**	**0.064**	**0.051**	**0.061**

The results in Tables 8 and 9 show that the Waterloo approach produces acceptable results when F_{yft} is used in place of F_y in the S136 expression. The average load ratios of all sections given in column 6 of Table 8 show an improvement of the yield load prediction of approximately 1% over the AISI load ratios shown in column 5. The results in column 5 of Table 9 show the reverse, i.e., that the AISI approach predicts a yield load that is approximately 1% better than the Waterloo approach. Based on the Waterloo test results, it was therefore concluded that the use of F_{yft} in place of the F_y term in the S136 expression produces results that are in excellent agreement with the AISI approach.

Table 9 - Comparison of Measured to Calculated Load Ratios of Tension Specimens

Specimen Identification	P_t (kN)	A_g (mm²)	P/P_y (1)	$P/P_{c(S136)}$ (2)	$P/P_{c(AISI)}$ (3)	$P/P_{cf(AISI)}$ (4)	P/P_{wat} (5)
H-2	90.8	217	1.06	1.01	1.01	0.99	1.00
H-3	74.2	216	1.15	1.09	1.08	1.04	1.05
H-4	70.0	208	1.06	1.01	1.00	1.00	1.01
C-1	183	342	1.14	1.08	1.06	1.05	1.06
		Mean	**1.10**	**1.05**	**1.04**	**1.02**	**1.03**
		Standard Deviation	**0.044**	**0.041**	**0.038**	**0.027**	**0.031**
		Coefficient of Variation	**0.04**	**0.039**	**0.037**	**0.026**	**0.030**
LC-1	146.3	349	1.37	1.16	1.17	1.04	1.08
LC-2	79.3	183	1.32	1.14	1.15	1.05	1.09
LC-3	154.3	445	1.23	1.04	1.07	1.02	1.01
		Mean	**1.31**	**1.11**	**1.13**	**1.04**	**1.06**
		Standard Deviation	**0.061**	**0.054**	**0.045**	**0.023**	**0.041**
		Coefficient of Variation	**0.047**	**0.049**	**0.04**	**0.022**	**0.039**
U-1	206.7	395	1.18	1.11	1.11	1.03	1.04
U-2	274.3	529	1.15	1.04	1.05	1.02	1.02
U-3	364.7	796	1.13	1.02	1.03	1.01	1.00
U-4	439.7	846	1.11	1.02	1.03	0.99	0.99
U-5	426.7	913	1.14	1.02	1.04	1.02	1.02
		Mean	**1.14**	**1.04**	**1.05**	**1.02**	**1.03**
		Standard Deviation	**0.027**	**0.036**	**0.032**	**0.018**	**0.031**
		Coefficient Of Variation	**0.024**	**0.034**	**0.031**	**0.018**	**0.030**
Summary of All Specimens							
		Mean	**1.17**	**1.06**	**1.07**	**1.02**	**1.04**
		Standard Deviation	**0.092**	**0.052**	**0.051**	**0.023**	**0.026**
		Coefficient Of Variation	**0.079**	**0.048**	**0.048**	**0.023**	**0.026**

5.1 Conclusions [13]

Based on the Waterloo test results and the analysis presented herein, the conclusions of this project can be summarised as follows:

1. The Waterloo test results were in good agreement with Karren's results and Lind and Schroff's theory. The increase in yield strength due to cold work of forming is dependent upon F_{uv}/F_{yv}, r/t and the margin (F_{uv} - F_{yv}) in the flats, corners and full sections. Specifically, the increase in yield strength becomes greater as the F_{uv}/F_{yv} ratio increases and as the r/t ratio decreases. The yield strength due to cold work of forming also showed a tendency to increase as the margin (F_{uv} - F_{yv}) increased.
2. The Waterloo Test results compare well with the experimental results produced by Karren et al [5] [6] [7] of corners and flats. The flat elements are affected by cold work of forming to a lesser degree than the corners. Some element to element variations of the yield strength exists in the flats of cold formed members.
3. The AISI and S136 design approaches produce nearly identical results when only the virgin mechanical properties of the steel are used.
4. Yield strengths, calculated using either the AISI or the S136 approach, compare well with both the stub column and full section tensile test results. In compression, the yield strength is underestimated by approximately 2% and in tension by approximately 6% for both approaches.
5. When the tested yield strength of the flats (F_{yfl}) is used in the AISI equation, on average the calculated

yield strength increased by approximately 4% in compression and 5% in tension for all sections. This translates into an overestimation of the tested yield strength by approximately 2% in compression and an underestimation of approximately 2% in tension.

6. Using F_{yft} values in the S136 equation in place of F_y, produced F_y' values within 1% on average in compression and within 2% on average in tension of the F_{ya} values calculated using AISI.

5.2 Recommendations

Based on the research presented in this paper, two recommendations are made, one to CSA S136 [2] and one to AISI [1].

The recommendation to S136 [2] is to allow the use of tested yield strength values of the flats of cold formed sections in the current calculation of the yield strength F_y' for fully effective members.
The recommendation to AISI [1] is to adopt the more simple modified S136 approach.

5.3 Acknowledgements

The authors wish to thank the American Iron and Steel Institute for their financial support and sponsorship of this research project. We wish to also thank the following people who have provided invaluable technical guidance during the course of this research project: Mr. Jim Moses, Mr. Tom Trestain, Mr. Steven R. Fox and Dr. Lei Xu. Finally, we wish to thank the following people and their respective companies for having provided us with the materials for testing: Mr. John Pellegrino of Ridg-U-Rack Inc., North East, Pennsylvania, Mr. Jim Moses and Mr. Adam Nawrot of Unistrut Corp., Itasca, Illinois and Mr. Reinhold Nickel and Mr. Wayne Law of Brockhouse Canada Inc., Brampton, Ontario, Canada.

Notations

b = empirical coefficient in Karren's theoretical expression
m = empirical coefficient in Karren's theoretical expression (or as stated below)
a = inside bend radius used in Karren's theoretical expression
t = material thickness
k = strength coefficient
σ_{ys} = full section yield strength
σ_{yc} = corner yield strength
σ_{yf} = yield strength of flats (from testing)
C = ratio of corner area to entire section area
F_{ya} = average yield point of the steel
F_{yf} = weighted average tensile yield point of the flats
F_{yc} = $B_c F_{yv}/(R/t)^m$, tensile yield point of corners.
B_c = $3.69\ (F_{uv}/F_{yv}) - 0.819(F_{uv}/F_{yv})^2 - 1.79$
m = $0.192\ (F_{uv}/F_{yv}) - 0.068$
R = inside bend radius
F_{yv} = tensile yield point of virgin steel
F_{uv} = ultimate tensile strength of virgin steel
f_u = alternate form of expressing the ultimate tensile strength
f_y = alternate form of expressing the yield strength
F_y = tensile yield strength
F_u = ultimate yield strength of steel
ΔP = increase in yield force
F_y = virgin yield strength of steel
D_A = number of 90° corners or total number of degrees in the section divided by 90°
w = centre line length of all or a portion of a section

W^* = ratio of centreline length to the thickness of all or a portion of a section (w/t)
P_t = tested load
P_c = calculated load
F_{yft} = average yield strength of the flats determined by testing
F_{uft} = average ultimate strength of the flats determined by testing
L = the overall length of a specimen,
r = radius of gyration about weak axis (typically y)
d = depth of section (measured parallel to web).
P_{yv} = the yield load of a specimen without influence from any type of buckling
P_{yeff} = the yield load of a specimen when local and/or distortional buckling is considered.
P_{cf} = an approximation of the yield load calculated when cold work of forming is considered
A_{eff} = effective area of section
A_g = gross area of section
P_{wat} = load calculated using the Waterloo approach

References

1. American Iron and Steel Institute, Cold-Formed Steel Design Manual, Part I-Dimensions and Properties, Part V-Specification, Part VI-Commentary, Part VII-Supplementary Information, Part VIII-Test Procedures, Washington, D.C., USA, 1996.
2. CSA S136-94, "Cold Formed Steel Structural Members," Canadian Standards Association, Rexdale (Toronto), Ontario, Canada, 1994.
3. LeMay, I., "Principles of Mechanical Metallurgy," Department of Mechanical Engineering, University of Saskatchewan, Elsevier, New York, (1981).
4. Flinn, R.A. and Trojan, P.K., "Engineering Materials and Their Applications," Third Edition, Houghton Mifflin Company, Boston, Massachusetts., 1986.
5. Chajes, Alexander, Britvec, S.J., and Winter, G., " Effect of Cold-Straining on Structural Steels," Journal of the Structural Division, ASCE, Vol.89, No. ST2, Proc. Paper 3477, April, 1963.
6. Karren, K.W., "Corner Properties of Cold Formed Steel Shapes," Journal of the Structural Division, ASCE, Vol. 92, No. ST1, Proc. Paper 5112, February, 1967.
7. Karren, K.W., and Winter, G., "Effects of Cold-Forming on Light-Gage Steel Members," Journal of the Structural Division, ASCE, Vol. 92, No. ST1, Proc. Paper 5113. February, 1967.
8. Lind, N.C., and Schroff, D.K., "Utilization of Cold Work in Light Gage Steel," Journal of the Structural Division, ASCE, Vol. 101, ST1, January, 1975.
9. ASTM E 8M-98, "Standard Test Methods for Tension Testing of Metallic Materials [Metric]," American Society for Testing and Materials, 1998.
10. ASTM E 9-89a, "Standard Test Methods of Compression Testing of Metallic Materials at Room Temperature," American Society for Testing and Materials (Reapproved 1995), 1995.
11. Hancock, G.J., "Design of Cold-Formed Steel Structures," Second Edition, Australian Institute of Steel Construction, 1994.
12. Rogers, C.A., "Local and Distortional Buckling of Cold Formed Steel Channel and Zed Sections in Bending," A thesis presented to the University of Waterloo for the degree of Master of Applied Science in Civil Engineering, Waterloo, Ontario, Canada, 1995.
13. Sloof, P.A., "Yield Strength Increase of Cold Formed Sections Due to Cold Work of Forming," A thesis presented to the University of Waterloo for the degree of Master of Applied Science in Civil Engineering, Waterloo, Ontario, Canada, 1999.